JOURNAL OF PETROLOGY | VOLUME 45 | NUMBER 11 | PAGES 2133–2153 | 2004 | doi:10.1093/petrology/egh050

Late-Stage Mafic Injection and Thermal Rejuvenation of the Vinalhaven Granite, Coastal Maine

R. A. WIEBE[1]*, M. R. MANON[2], D. P. HAWKINS[3] AND W. F. McDONOUGH[4]

[1]DEPARTMENT OF EARTH AND ENVIRONMENT, FRANKLIN AND MARSHALL COLLEGE, LANCASTER, PA 17604-3003, USA

[2]DEPARTMENT OF GEOLOGICAL SCIENCES, UNIVERSITY OF MICHIGAN, ANN ARBOR, MI 48109-1063, USA

[3]DEPARTMENT OF GEOLOGY AND GEOGRAPHY, DENISON UNIVERSITY, GRANVILLE, OH 43023, USA

[4]DEPARTMENT OF GEOLOGY, UNIVERSITY OF MARYLAND, COLLEGE PARK, MD 20742, USA

RECEIVED DECEMBER 10, 2003; ACCEPTED JUNE 11, 2004
ADVANCE ACCESS PUBLICATION AUGUST 19, 2004

The Vinalhaven intrusive complex consists mainly of coarse-grained granite, inward-dipping gabbro–diorite sheets, and a fine-grained granite core. Small bodies of porphyry occur throughout the coarse-grained granite. The largest porphyry body (roughly 0·5 km by 2·5 km) occurs with coeval gabbro, hybrid rocks, and minor fine-grained granite in the Vinal Cove complex, which formed during the waning stages of solidification of the coarse-grained Vinalhaven granite. Porphyry contacts with surrounding coarse-grained granite are irregular and gradational. Compositions of whole rocks and minerals in the porphyry and the coarse-grained granite are nearly identical. Neighboring phenocrysts in the porphyry vary greatly in degree of corrosion and reaction, indicating that the porphyry was well stirred. Thermal rejuvenation of a silicic crystal mush by a basaltic influx can explain the composition and texture of the porphyry. Comparable rejuvenation events have been recognized in recent studies of erupted rocks. Weakly corroded biotite phenocrysts in the porphyry require that hydrous interstitial melt existed in the granite during remelting. Field relations, along with thermal calculations, suggest that cooling and crystallization of coeval mafic magma could have generated the porphyry by thermal rejuvenation of granite crystal-mush containing about 20% melt. Field relations also suggest that some of the porphyry matrix may represent new felsic magma that was emplaced during remelting.

KEY WORDS: *granite; magma chamber; mafic replenishment; rejuvenation*

INTRODUCTION

Volcanic and plutonic rocks provide complementary records of magma chamber evolution in the crust. Volcanic studies have long made many important contributions to our understanding of magma chamber processes, including concepts of multiple replenishment, mixing and fractionation of magmas. Although there is abundant evidence that many shallow-level granitic plutons were the source of associated volcanic sequences, studies of granites have not commonly focused on magma chamber processes. None the less, these bodies should be able to provide valuable corroborating evidence about processes inferred from volcanic studies and, perhaps, even provide new insights. For example, the recognition from volcanic studies of the importance of mafic replenishments in silicic magma chambers (Sparks *et al.*, 1977; Murphy *et al.*, 2000) is now widely supported by the occurrence of extensive comagmatic sheets of mafic rocks in many plutons (e.g. Wiebe, 1974, 1994; Michael, 1991; Coleman *et al.*, 1995; Patrick & Miller, 1997). Recently, a number of volcanic studies have inferred that injections of higher temperature magma can cause thermal rejuvenation of a nearly solidified plutonic mass. Is it possible to find a complementary record of similar rejuvenation in a granitic pluton?

Mafic injections into granite or a silicic magma chamber may react in different ways depending on the crystallinity and, hence, the rheology, of the silicic material the injected magma encounters, as well as the total volume and rate of flow of the mafic magma. If the granitic material were solid and cold (e.g. <300°C), then one would expect simple dikes with little or no remelting of

*Corresponding author. E-mail: bwiebe@fandm.edu

the adjacent granite. As the temperature of the host granite approaches its solidus, the effect of heating from the basalt would be expected to cause some marginal melting, which might be indicated by simple 'back-veining'. As temperatures rise above the granite solidus, the strength of the adjacent granite may drop rapidly as melting occurs, and the mafic dikes may begin to break down into either brittle or pillow-like segments characteristic of synplutonic dikes (Pitcher, 1991).

Assuming that most granitic plutons crystallize from their margins inward, it should be common for basaltic magma to pass inward through a solid margin to an interior of decreasing crystallinity. Evidence for this transition is provided by many intrusions that contain mafic layers that have ponded on a crystal-rich granitic mush at the base of a crystal-poor chamber (Wiebe, 1974, 1993a; Wiebe & Collins, 1998). Heat from these mafic layers has commonly remobilized the underlying, less dense crystal mush. The changing rheology of the granitic crystal mush and the density inversion may cause load-casts of the denser basaltic material to develop in the underlying crystal mush and diapiric upwelling of that mush through the mafic layer (Wiebe & Collins, 1998).

At some times and places within a silicic magma chamber, there should exist a substantial volume of stagnant, crystal-rich mush of intermediate rheology that, when energized by a basaltic replenishment, can be transformed into a mobile magma capable of erupting. Evidence for this remobilization of crystal-rich mush has recently been recognized in both small and large eruptive systems (Murphy *et al.*, 2000; Bachmann *et al.*, 2002).

Several bodies of felsic porphyry occur in the Vinalhaven intrusive complex and have gradational and irregular contacts with the enclosing coarse-grained Vinalhaven granite. The largest of these bodies is commingled and locally mixed with a contemporaneous basaltic injection. The felsic porphyry has a whole-rock composition essentially identical to the granite and contains highly corroded phenocrysts with compositions that match those of crystals in the granite. These bodies of porphyry appear to be the plutonic record of thermal rejuvenation comparable with that inferred from erupted rocks (Keller, 1969; Murphy *et al.*, 2000; Allen, 2001; Couch *et al.*, 2001; Bachmann *et al.*, 2002). Widespread evidence for quenching of silicic magma in this plutonic environment suggests that these rejuvenated magma chambers may have been connected to eruptions. The purpose of this paper is to document this first recognized occurrence of thermal rejuvenation within a granitic pluton.

GEOLOGICAL SETTING

Vinalhaven Island is located in southern Penobscot Bay, about 15 km east of Rockland, Maine (Fig. 1). The plutonic rocks on Vinalhaven Island belong to the Coastal Maine Magmatic Province (Hogan & Sinha, 1989), an association of more than 100 bimodal granite–gabbro plutons, which intruded parallel to NE-trending, fault-bounded terranes from the Late Silurian to Early Carboniferous (Hogan & Sinha, 1989). The terranes consist primarily of pre-Devonian meta-volcanic and meta-sedimentary rocks, and are thought to be microplates of continental crust that accreted onto the North American craton during the Acadian Orogeny (Hogan & Sinha, 1989). Hogan & Sinha (1989) proposed that magmatism in the Coastal Maine Magmatic province is related to rifting in a transtensional environment where crustal extension and lithospheric thinning allowed for the emplacement of mafic magma at various crustal levels. A subsequent shift to a transpressional regime is thought to have trapped mafic magma at the base of the crust and induced partial melting of the overlying granitic crust.

Many dominantly granitic plutons of the Coastal Maine Magmatic Province contain variable proportions of contemporaneous mafic rocks (Wiebe, 1996), and the Vinalhaven plutonic rocks are typical of these bimodal complexes. Hawkins *et al.* (2002) reported a U–Pb zircon date of 420 ± 1 Ma from the Vinalhaven granite, an age essentially identical to that of the Cadillac Mountain intrusive complex (Seaman *et al.*, 1995).

THE VINALHAVEN INTRUSIVE COMPLEX

The Vinalhaven intrusive complex was emplaced mainly into deformed, low-grade schists of the early Paleozoic Calderwood Formation and, along its northwestern margin, into weakly deformed Silurian volcanic rocks that include rhyolitic rocks contemporaneous with the intrusion (Hawkins *et al.*, 2002; Hawkins and Wiebe, 2005) (Fig. 1).

The complex consists of three main units [coarse-grained (cg) granite, gabbro–diorite and fine-grained (fg) granite] and several smaller bodies of felsic porphyry (Fig. 1). The most extensive unit is coarse-grained granite, which underlies most of the island and has a well-exposed contact with country rock along its northern (upper) margin. In the SE half of the complex, the coarse-grained granite is underlain by a gabbro–diorite unit, which consists of interlayered mafic, hybrid, and granitic rocks. This unit forms a curved, sheet-like body, hundreds of meters to >1 km thick, which dips 10–30° to the north and west beneath the granite. Extensive blocks of country rock, identical to country rock in the northern part of the island, occur within the gabbro–diorite unit. Metamorphism of pelitic blocks suggests pressures of between 1 and 2 kbar (Porter *et al.*, 1999). Younger, fine-grained granite cuts through the gabbro–diorite unit and forms a small, inner core of the intrusion, about 2–3 km in diameter, mainly within the coarse-grained granite.

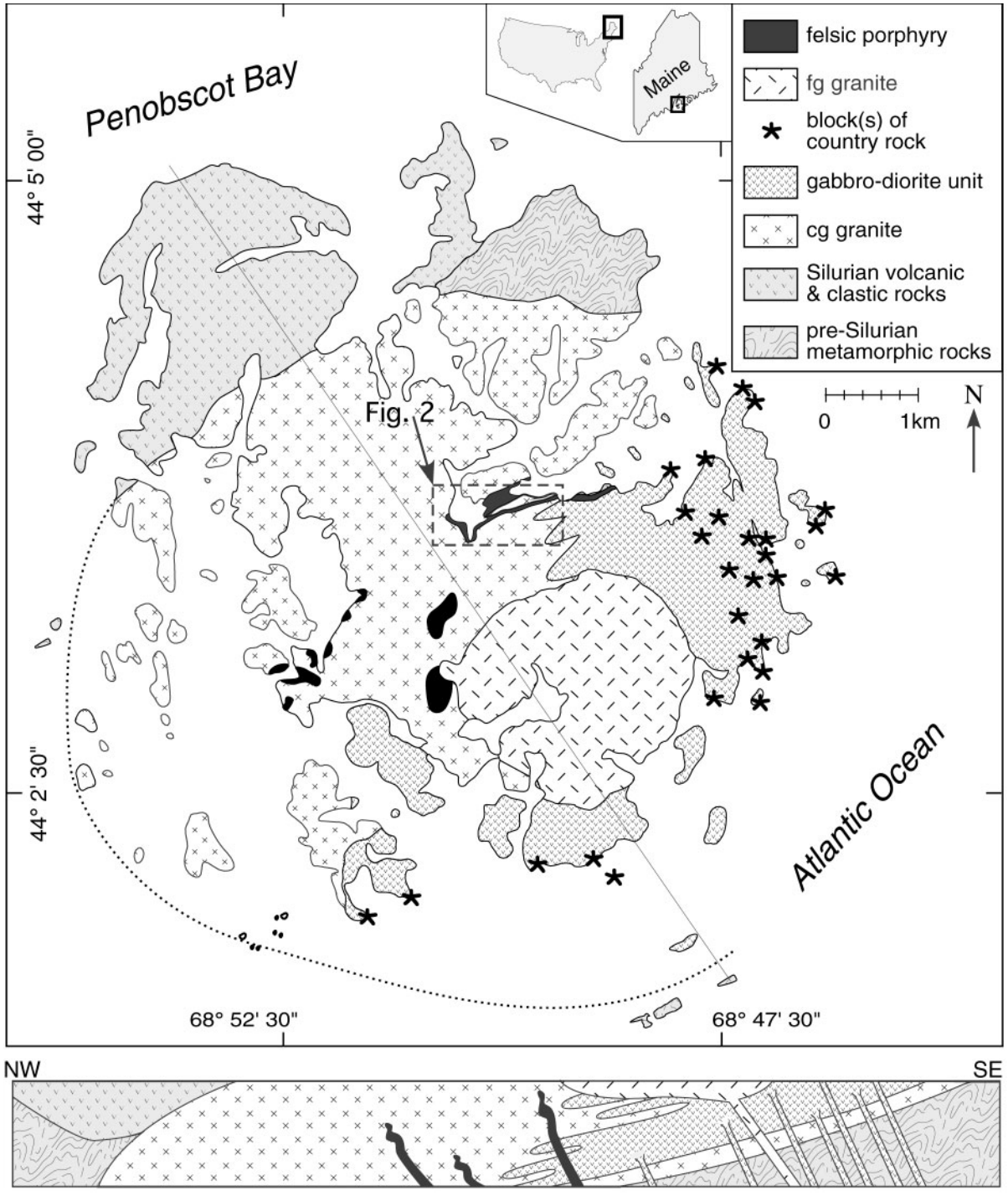

Fig. 1. Geological map and cross-section of the Vinalhaven intrusion, Vinalhaven Island, Penobscot Bay, Maine.

Much of the gabbro–diorite can be subdivided into macro-rhythmic units (layers), each of which is marked by a chilled gabbroic base. These macro-rhythmic units may vary in thickness from <1 m to >100 m. Where gabbroic rocks form layers less than a few meters thick, they commonly have chilled upper margins against a more felsic, overlying layer that is compositionally similar to rocks beneath the sheet. Where gabbroic rocks form layers thicker than a few meters, they generally grade upward to hybrid dioritic and even granitic rocks that

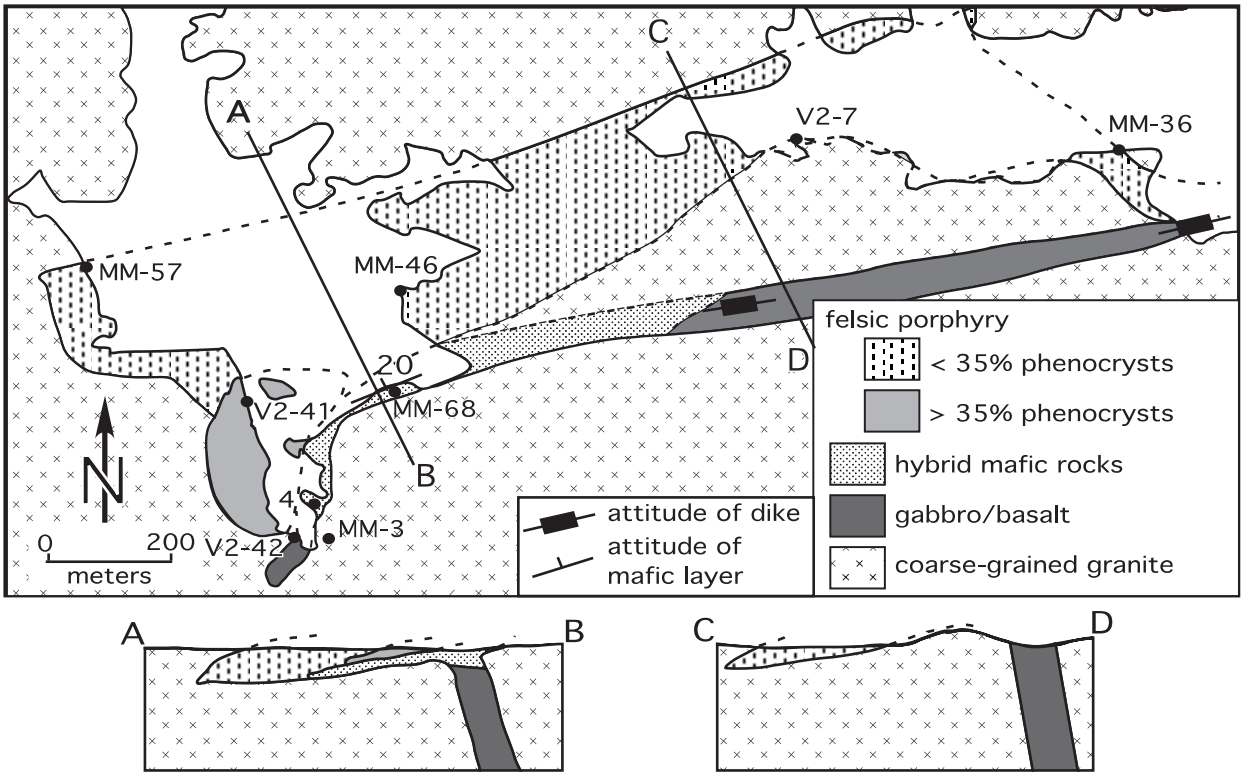

Fig. 2. Geological map and schematic cross-sections of the Vinal Cove complex. Contacts between gabbro/basalt and hybrid mafic rocks and between the two porphyry units are gradational. Points with numbers refer to locations listed in the text and shown in other figures.

display evidence for incomplete mixing between mafic and felsic magmas. Widespread load-cast and pipe structures at the chilled mafic bases of macrorhythmic units are consistent with the gabbro–diorite unit being formed by a sequence of basaltic injections that ponded at the base of an aggrading silicic magma chamber and variably interacted with overlying granitic magma (Wiebe, 1993*a*; Wiebe & Collins, 1998).

In addition to these well-defined macro-rhythmic layers, the gabbro–diorite unit also includes areas of tightly packed sheets, tubes, and pillows of chilled gabbroic rocks in a granitic to hybrid matrix. These areas of commingled rocks appear to be eroded remnants of mounds, up to >10 m high and 100 m in diameter (Wiebe *et al.*, 2001). Many pillow mounds appear to grade to the more massive thicker macro-rhythmic units, suggesting that some mounds are flow fronts to large mafic replenishments.

Several areas of felsic porphyry occur within the coarse-grained granite. Contacts between porphyry and the enclosing coarse-grained granite are typically gradational over a few centimeters and, commonly, highly irregular with mutually intrusive relations. Minor segments of the contacts of some porphyry bodies appear to sharply cut across crystals in coarse-grained granite. The porphyry is characterized by varying abundances of corroded and reacted phenocrysts of quartz, alkali feldspar, plagioclase and biotite in a fine-grained to aphanitic, felsic matrix. It commonly contains a few percent of variably chilled mafic enclaves from a few millimeters to several centimeters in diameter; larger bodies of mafic rock are associated with some porphyries. The largest body of porphyry occurs in the Vinal Cove complex (Fig. 2), which appears to be the last active magma chamber of the Vinalhaven intrusive complex.

FIELD RELATIONS IN THE VINAL COVE COMPLEX

The Vinal Cove complex is dominated by felsic porphyry and contains a substantial volume of contemporaneous gabbroic and hybrid mafic rocks (Fig. 2). A steeply dipping dike of olivine gabbro, up to about 80 meters thick, trends about N75°E along part of the southern margin of the complex. It grades along its length to a curved central area of hybrid mafic rocks, which, along its NW margin, is in contact and commingled with the felsic porphyry. The homogeneous western and eastern gabbroic ends of the dike are strongly chilled against cg granite. Near the SW end of the gabbro dike (locality V2-42), a strongly chilled margin of the gabbro is separated from the

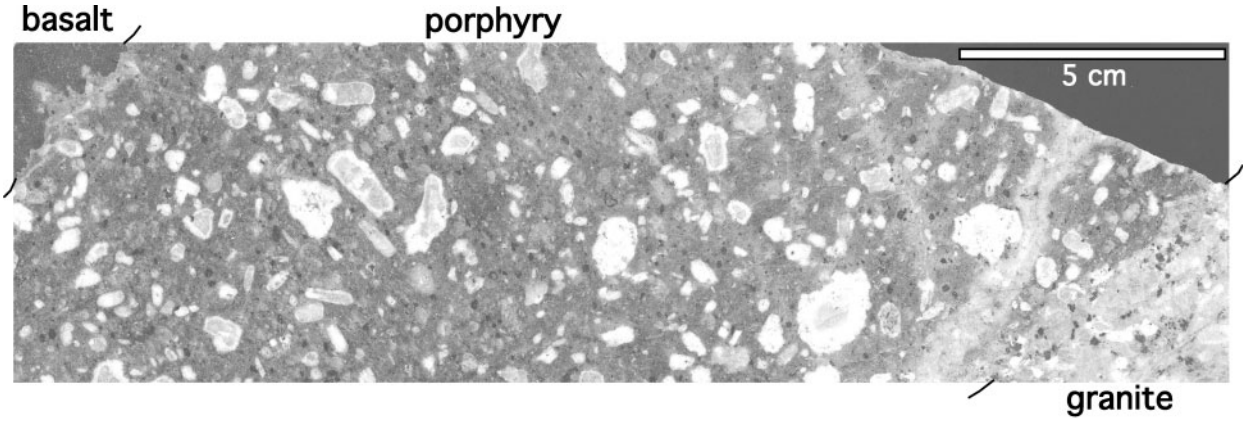

Fig. 3. Contact between cg granite (on right) and basaltic dike (on left) at locality V2-42. A porphyry layer of 20 cm thickness with an aphanitic matrix separates basalt from granite. The basalt is strongly chilled and has an irregular crenulate margin against the porphyry. The porphyry contains about 20% highly corroded phenocrysts of quartz, feldspar and biotite, as well as scarce small quenched mafic droplets. White plagioclase rims are apparent on several gray alkali feldspar crystals near the margin of the basaltic dike.

coarse-grained Vinalhaven granite by about 20–30 cm of porphyry with an aphanitic matrix (Fig. 3). The contact between the 'basalt' and the porphyry is highly irregular and crenulate. The contact between the porphyry and the granite is gradational over a distance of <1 cm.

A composite dike of 2–4 m thickness, consisting of chilled gabbroic pillows in fine-grained, aphyric granite, cuts irregularly through the gabbro and felsic to hybrid porphyry near locality 4 (Fig. 2). The mafic component of the dike is nearly identical in composition to the main gabbro dike and appears to be a slightly later pulse of similar magma. The fine-grained granite host, similar in composition to both the porphyry and the coarse-grained granite, may represent new input of felsic magma. Similar composite dikes of chilled gabbroic pillows in fine-grained granite occur in all of the coeval intrusions along the Maine coast (Snyder *et al.*, 1997). They appear to represent the common, though yet unexplained, tendency for both mafic and silicic inputs to occur at the same time.

The unit of hybrid mafic rocks is extremely heterogeneous in texture and composition, and includes minor amounts of felsic porphyry. Hybrid mafic rocks appear to grade eastward to the homogeneous gabbro dike. Coastal exposures display highly irregular contacts between hybrid mafic rocks and felsic porphyry. Exposures in the SW part of this complex, near locality MM-68, contain several examples of hybrid mafic sheets with basal load casts in underlying, heterogeneous, crystal-rich porphyry. Steeply SE-plunging granitic pipes occur in these mafic rocks. Because such silicic pipes appear to record the vertical direction at the time of their emplacement (Wiebe & Collins, 1998), and because they are generally perpendicular to the mafic sheets in which they occur (Wiebe, 1993b), their orientations suggest that the sheets dip about 20°NW beneath the main area of porphyry.

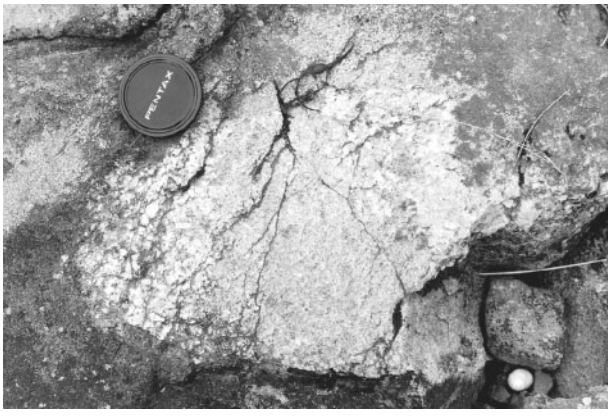

Fig. 4. A rounded block of coarse-grained granite in hybrid mafic rocks (locality MM-68). Feldspar and quartz xenocrysts in the mafic rock (lower left) appear to have been incorporated from the partially remelted granite.

Blocks of cg granite occur in the mafic rocks (Fig. 4), and felsic porphyry and hybrid mafic rocks are locally commingled. Large globular masses of chilled gabbro in hybrid felsic porphyry occur at locality 4. Some hybrid mafic rocks contain both strongly chilled mafic enclaves, and feldspar and quartz xenocrysts.

The map unit of felsic porphyry appears to be a sheet-like mass that dips gently to the NNW above the mafic hybrid rocks. It is characterized by corroded phenocrysts of quartz, alkali feldspar, plagioclase and biotite that are comparable in size with crystals in the cg granite. The percentage of phenocrysts is greatest near the southern (lower) part of the porphyry unit and decreases toward the northern (upper) contact (Fig. 2; Table 1). Contacts of the porphyry with the surrounding cg granite are gradational over distances of about 1–10 cm and typically highly irregular (Fig. 5). A felsic dike of 2 m thickness

*Table 1: Modes of porphyry from the Vinal Cove complex**

Sample:	V2-42B1	V2-42B2	V2-42B3	V2-7	V2-41	MM-2	MM-57	MM-36
Matrix	70·5	67·9	69·2	81·3	63·0	61·7	87·8	68·0
Plagioclase	9·9	16·5	12·5	8·5	23·0	21·0	2·6	23·9
K-feldspar	8·8	4·9	4·5	5·6	8·3	10·5	4·7	0·0
Quartz	9·7	9·6	12·5	2·9	2·8	4·4	3·3	6·7
Biotite	0·9	0·9	1·1	0·2	0·8	1·4	0·4	0·0
Hornblende	0·2	0·2	0·2	0·3	0·3	0·2	0·5	0·8
Allanite	0·0	0·0	0·0	0·0	0·2	0·0	0·0	0·0
Mafic encl.	0·0	0·0	0·0	1·2	1·6	0·8	0·7	0·7
No. of points	1171	1451	1316	1075	1067	987	1024	1031

*Grid of points is 1·0 mm by 0·5 mm.

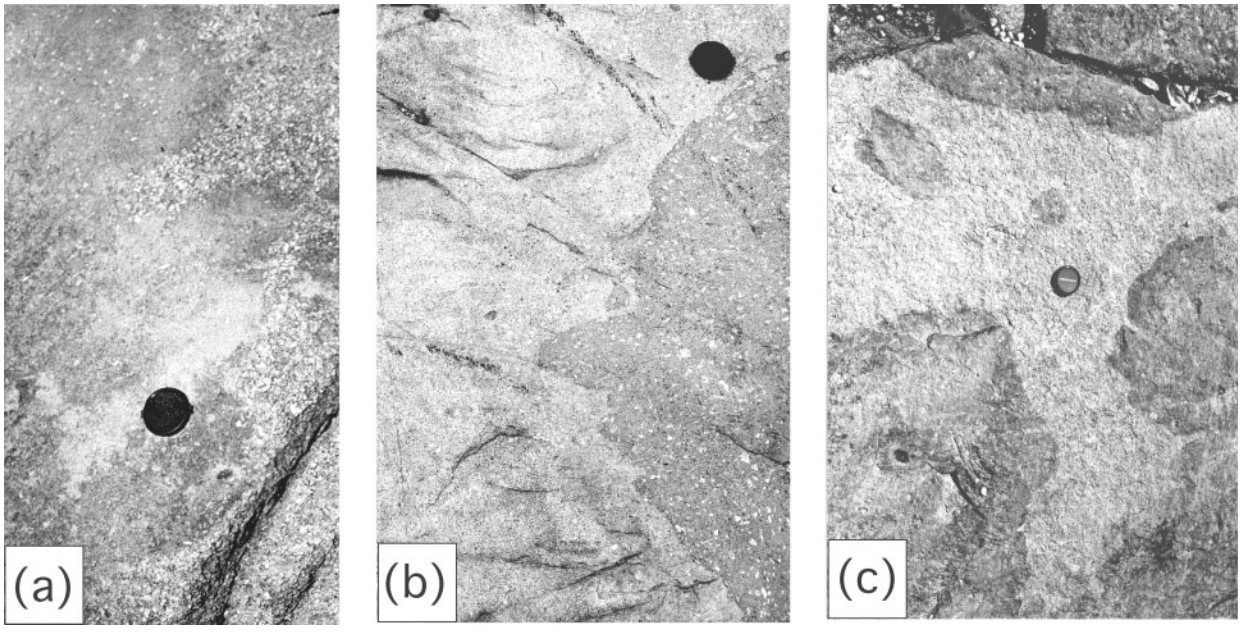

Fig. 5. Contacts between porphyry of the Vinal Cove complex and the enclosing coarse-grained Vinalhaven granite. (a) Irregular and gradational contact of porphyry (left) and granite (right). Crystals are disaggregated along the edge of the granite. (b) Irregular but sharp contact of granite (left) and porphyry (right). (c) Commingling of granite (light) and porphyry (dark). Small veinlets of granite have penetrated into rounded masses of porphyry. These suggest that, during emplacement, the porphyry became solid enough to fracture, permitting interstitial melt from the granite to form veins in it.

with 10–20 cm marginal bands of spherulitic plagioclase (up to 1 cm in diameter) extends from the northern (upper) margin of the porphyry into the granite.

Within the map area of Fig. 2, the porphyry never cuts across crystals in the granite, suggesting that the cg granite retained interstitial melt when the porphyry intruded. Dikes of the porphyry at the far eastern end of the Vinal Cove complex (east of the area shown in Fig. 2) do cut across crystals in the granite sharply, indicating that coarse-grained granite was effectively solid further away from the major area of porphyry.

ANALYTICAL METHODS

Analyses of major elements in feldspars and biotite were performed on a JEOL 8900 Superprobe at the Center for Microscopy and Microanalysis at the University of Maryland. Analyses were obtained using the following analytical conditions: accelerating voltage of 15 keV, sample current of 10 nA, and a beam diameter of 5 nA. Peak and background intensities were measured for all elements; raw intensities were corrected using a CIT-ZAF algorithm. Orthoclase (K, Ba), albite (Na), plagioclase (Ca, Al, Si) and hornblende (Ti, Fe) were used as standards for

Table 2: Representative major element analyses of feldspar cores from the coarse-grained Vinalhaven granite and Vinal Cove porphyry

Rock type:	Plagioclase in cg Vinalhaven granite						Plagioclase in porphyry					
Sample:	MM-62A	MM-62A	MM-62A	V-002	V-002	V-002	MM-53	MM-53	MM-53	MM-46	MM-46	MM-46
SiO_2	61·67	62·03	64·11	62·04	62·21	63·28	62·52	62·98	64·40	62·34	62·71	64·03
TiO_2	0·03	0·04	0·05	0·02	0·04	0·07	0·08	0·03	0·03	0·02	0·03	0·07
Al_2O_3	24·75	24·03	22·75	23·17	23·83	23·15	23·79	23·13	22·10	24·10	23·30	23·25
FeO	0·24	0·21	0·28	0·17	0·19	0·21	0·20	0·08	0·16	0·23	0·23	0·20
CaO	6·37	5·76	3·82	5·67	5·35	4·77	5·47	4·78	3·85	5·78	5·16	4·65
Na_2O	8·01	8·23	9·01	8·08	8·27	8·56	8·31	8·56	8·81	7·90	8·12	8·72
K_2O	0·28	0·50	0·34	0·35	0·45	0·46	0·42	0·45	0·67	0·58	0·61	0·41
BaO	0·03	0·00	0·05	0·00	0·02	0·02	0·03	0·00	0·00	0·05	0·00	0·01
Total	101·39	100·80	100·40	99·50	100·36	100·52	100·81	100·01	100·00	100·99	100·16	101·36
%An	30·0	27·1	18·6	27·4	25·6	22·9	26·0	23·0	18·7	27·8	25·1	22·2
%Ab	68·4	70·1	79·5	70·6	71·8	74·4	71·6	74·5	77·5	68·8	71·4	75·4
%Or	1·6	2·8	1·9	2·0	2·6	2·6	2·4	2·6	3·9	3·3	3·5	2·4

Rock type:	Alkali feldspar in cg Vinalhaven granite						Alkali feldspar in porphyry					
Sample:	MM-62A	MM-62A	MM-62A	V-002	V-002	V-002	MM-53	MM-53	MM-53	MM-46	MM-46	MM-46
SiO_2	65·34	65·19	64·88	65·31	65·04	65·64	64·64	65·30	64·99	64·76	65·03	65·30
TiO_2	0·03	0·01	0·03	0·01	0·04	0·05	0·05	0·05	0·06	0·41	0·03	0·06
Al_2O_3	18·43	18·27	18·76	18·91	18·77	18·61	18·82	18·85	18·57	18·86	18·82	18·79
FeO	0·07	0·01	0·00	0·09	0·07	0·06	0·01	0·00	0·09	0·09	0·08	0·04
CaO	0·00	0·03	0·02	0·08	0·04	0·01	0·06	0·00	0·04	0·18	0·02	0·09
Na_2O	0·58	0·58	0·59	0·74	0·66	0·62	0·67	0·34	0·29	0·84	0·30	0·61
K_2O	15·64	15·55	15·71	15·10	15·31	15·20	15·42	15·52	15·64	14·93	15·72	15·38
BaO	0·10	0·00	0·04	0·15	0·15	0·20	0·31	0·03	0·13	0·27	0·12	0·28
Total	100·19	99·64	100·02	100·39	100·09	100·39	99·98	100·09	99·81	100·34	100·13	100·54
%An	0·0	0·2	0·1	0·4	0·2	0·1	0·3	0·0	0·2	0·9	0·1	0·5
%Ab	5·4	5·4	5·4	6·9	6·2	5·8	6·2	3·2	2·8	7·8	2·8	5·7
%Or	94·6	94·4	94·5	92·7	93·6	94·1	93·5	96·8	97·0	91·3	97·1	93·9

the feldspar analyses. Phlogopite (K, Mg, Fe, Ti, Al, Si, F), Fe-rich biotite (Cl), albite (Na), and ilmenite (Mn) were used as standards for the biotite analyses. Representative compositions of feldspars and biotite determined by electron microprobe are listed in Tables 2 and 3.

Trace elements in feldspars and biotite were determined by laser ablation inductively coupled plasma mass spectrometry (LA-ICP-MS) at the University of Maryland. The laser system, a frequency quintupled Nd:YAG that delivers 213 nm light (UP213 from New Wave Research), is coupled to an Element 2 (Thermo Finnigan MAT) magnetic sector ICP-MS system, equipped with a fast magnet scanning option. Throughout the analyses the ablation cell is continuously flushed with He ($\sim$0·8 ml/min). This He gas stream, along with its entrained ablated materials, is later mixed with Ar ($\sim$0·6 ml/min) in a small volume (0·5 cm^3) chamber before it enters the plasma. Laser spot sizes ranged from $\sim$30 to $\sim$60 μm and together with the laser repetition rate (3–8 Hz) were set to optimize maximum signal intensity to $\sim$106 c.p.s. A single mass scan of 25–30 elements was acquired over 0·38–0·40 s in syncro-scan mode; this mode provides a stable combination of magnet jumps and voltage scans of the electrostatic analyzer while minimizing the acquisition period. Time-resolved spectra included the acquisition of $\sim$20 s of gas background

Table 3: Representative analyses of biotite cores from the coarse-grained Vinalhaven granite and Vinal Cove porphyry

Rock type:	cg Vinalhaven granite				Porphyry			
Sample:	MM-62A	MM-62A	V-002	V-002	MM-53	MM-53	MM-46	MM-46
SiO_2	35·75	35·98	35·42	35·75	36·43	37·19	36·07	36·52
TiO_2	3·96	3·99	3·61	3·79	3·87	3·62	3·81	3·84
Al_2O_3	13·28	13·01	14·93	15·02	12·82	13·30	13·21	13·27
FeO	26·71	24·77	22·19	21·54	23·60	23·22	23·97	23·90
MnO	0·61	0·49	0·41	0·47	0·32	0·26	0·36	0·42
MgO	7·19	7·47	9·62	9·94	9·71	10·34	9·32	9·22
Na_2O	0·00	0·08	0·09	0·13	0·05	0·04	0·06	0·09
K_2O	9·70	9·86	9·93	9·97	9·88	9·71	9·96	9·96
F	0·98	0·77	0·88	0·91	0·94	1·15	1·05	1·02
Cl	0·16	0·10	0·17	0·15	0·10	0·11	0·13	0·12
Total	97·90	96·16	96·84	97·26	97·31	98·43	97·46	98·01
Mg/(Mg + Fe)	32·4	35·0	43·6	45·1	42·3	44·3	40·9	40·7

followed by 40–80 s of signal. A series of analyses of unknowns were bracketed by the analyses of two NIST 610 glass standards before and after each series. Accuracy was monitored by repeat analyses of BCR-2 g throughout each session, with results being comparable with that reported by Barth *et al.* (2001). Time-resolved spectra were processed off-line using a modified version of LAMTRACE (S. E. Jackson). Concentration determinations and compensation for variations in ablation yields were corrected using an internal standard element (Ca for plagioclase, Ti for biotite and Ga for K-feldspar). Concentrations of Ca and Ti in plagioclase and biotite, respectively, were measured by electron microprobe. The Ga contents of K-feldspar were set at 21 ppm, based on an assumed constant Al/Ga value for K-feldspar. Minimum detection limits for reported concentrations are calculated based on 3σ above the background count rate.

Whole-rock samples were analyzed for major and trace elements by X-ray fluorescence (XRF) at Franklin and Marshall College using a Philips 2404 XRF vacuum spectrometer equipped with a 4 kW Rh X-ray tube. For major element analysis nine parts $Li_2B_4O_7$ was mixed with one part rock powder and fused into a homogeneous glass disk. Working curves were determined by analyzing 51 geochemical rock standards, data for each having been compiled by Govindaraju (1994). Analytical errors associated with measuring major element concentrations range from <1% for Si and Al to ~3% for Na. Trace element briquettes were prepared by mixing 7 g of whole-rock powder with 1·4 g of pure microcrystalline cellulose. Analytical errors for the trace elements range from 1–2% for Rb, Sr, Y, Zr, etc., to 5–6% for Ba.

PETROGRAPHY

Medium- to coarse-grained Vinalhaven granite, which encloses the Vinal Cove complex, is dominated by subhedral, weakly tabular, pink, perthitic alkali-feldspar (3–8 mm in diameter) with subordinate smaller, blocky white plagioclase and equant quartz (Fig. 6a). In many granite samples, these crystals occur within varying proportions (5–20%) of finer-grained interstitial quartz and feldspar. The mafic minerals consist mainly of biotite, locally with minor hornblende, and accessory Fe–Ti oxides, allanite, apatite, titanite and zircon. Plagioclase has delicate, oscillatory–normal zoning, mainly $An_{27–20}$ (Table 2). Alkali feldspar shows coarse perthitic exsolution and, uncommonly, faint subhedral zoning. In some areas, granites commonly contain up to a few percent of very fine-grained plagioclase–hornblende enclaves 2–10 mm in diameter.

Increasing amounts of fine-grained interstitial matrix between larger subhedral crystals commonly occur in the transition from granite into the Vinal Cove porphyry. Granite, within a few centimeters of the contact between hybrid porphyry and chilled gabbro, typically shows prominent, uniformly thick zones of microgranophyric quartz and feldspar between adjacent quartz and feldspar crystals, but not between adjacent plagioclase crystals (Fig. 7).

Fine-grained granite from the composite dike has a mineralogy and mode that closely resembles the coarse-grained granite, having roughly equal amounts of quartz, plagioclase and alkali feldspar between 0·1 and 1 mm in diameter with about 5% biotite and accessory Fe–Ti oxides, allanite, apatite, titanite and zircon. Scarce phenocrysts of quartz and both feldspars occur sparsely.

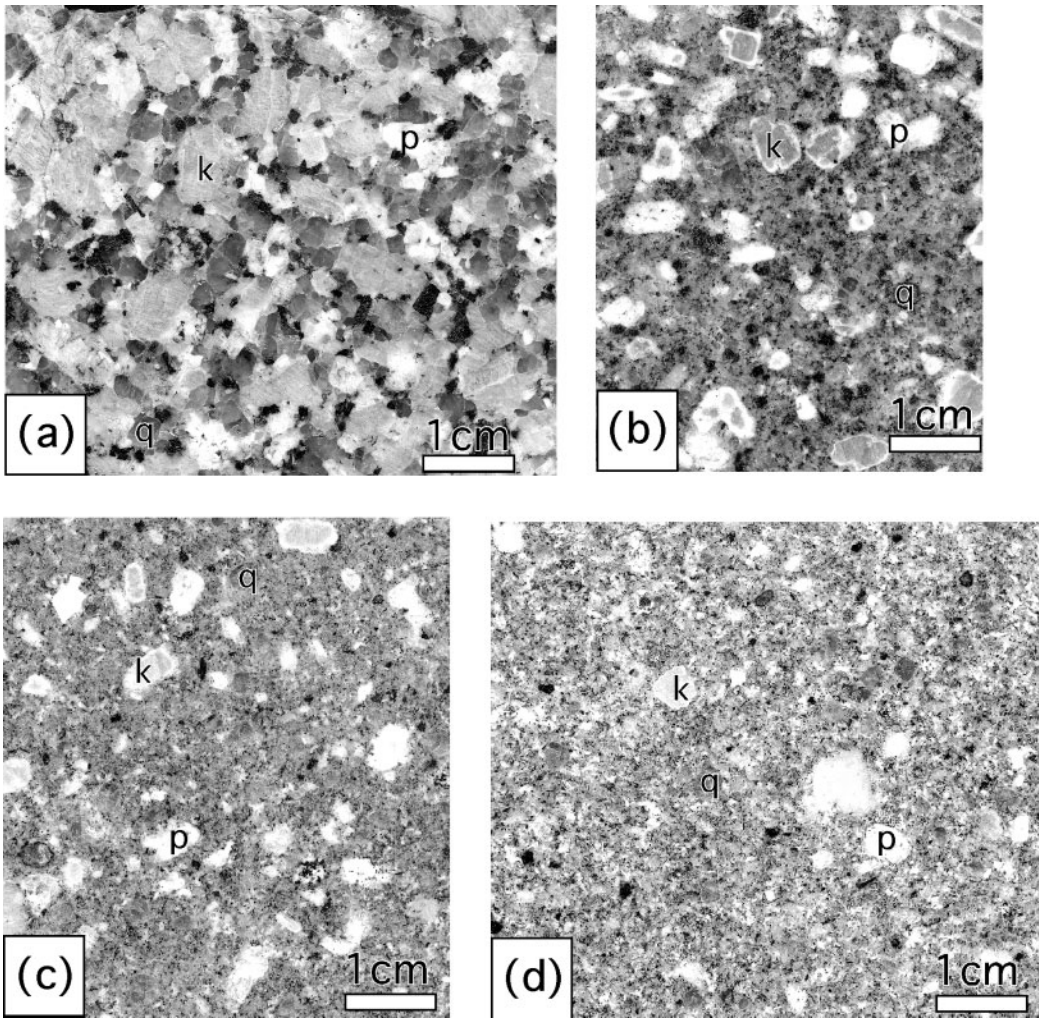

Fig. 6. Polished slabs of coarse-grained Vinalhaven granite and porphyry from the Vinal Cove complex. Representative phenocrysts are labeled as: plagioclase (p), alkali-feldspar (k) and quartz (q). Locations of all samples are shown in Fig. 2. (a) Coarse-grained Vinalhaven granite (locality MM-3). (b) Phenocryst-rich porphyry from the southern part of the complex (locality V2-41). White plagioclase rims of varying thickness occur on alkali feldspar phenocrysts. (c, d) Phenocryst-poor porphyry from the northern part of the complex (c, locality MM-46; d, locality MM-57).

The Vinal Cove porphyry has between 5 and 45% phenocrysts that are similar in identity, size and composition to minerals in the Vinalhaven granite (Table 1; Fig. 6b–d). Most phenocrysts are anhedral and appear to be highly corroded, and many have reaction rims. Adjacent crystals may vary greatly in their degree of corrosion and reaction. Alkali feldspar phenocrysts may be anhedral and lack plagioclase overgrowths or have plagioclase rims that vary in thickness from a few microns to about 1 mm (Fig. 8a and b). Plagioclase phenocrysts have compositions and zoning similar to that in the granite (Table 2), although plagioclase phenocrysts and plagioclase rims on K-feldspar commonly contain many patches of microgranophyric intergrowths of quartz and K-feldspar (Fig. 8b). The anhedral margins of plagioclase commonly truncate delicate oscillatory zoning, as do fretted rims (up to 300 μm thick) with minute quartz and alkali-feldspar inclusions. Some quartz phenocrysts have prominent hornblende ± biotite reaction rims, whereas other nearby phenocrysts lack rims and have poikilitic overgrowths of varying thickness into the matrix (Fig. 8c and d). Biotite phenocrysts are typically anhedral and commonly have poikilitic overgrowths that extend as much as 150 μm into the fine-grained matrix (Fig. 8e).

In some northern areas, the porphyry grades to fine-grained granite similar to that found in the composite dike. These rocks typically have less than 10% phenocrysts of feldspar and quartz that lack evidence of corrosion or reaction.

The grain size and textures of the porphyry matrix vary widely. The finest-grained matrix is aphanitic with acicular apatite and is dominated by microgranophyric

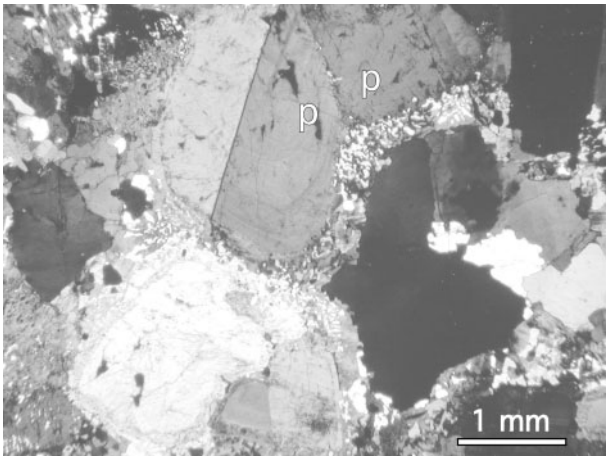

Fig. 7. Vinalhaven granite within 10 cm of the contact with porphyry. The granite has microgranular zones formed by crystallization of rejuvenated melt sheets. Microgranular zones occur along boundaries of quartz and feldspar in granite and are absent along plagioclase–plagioclase contacts (p p).

intergrowths of quartz and alkali-feldspar along with plagioclase and biotite (mostly 10–100 μm in diameter). More commonly, the matrix has coarser granophyric textures along with plagioclase crystals that are subequant and range from 50 to 300 μm in diameter. Microgranophyric textures also occur commonly as overgrowths on quartz (Fig. 8f).

The ~20 cm thick zone of porphyry that occurs between chilled gabbro and Vinalhaven granite at locality V2-42 (Fig. 2) has an aphanitic matrix with about 25–30% highly corroded phenocrysts of quartz, feldspar and biotite as well as scarce, small (1–5 mm) quenched mafic droplets. Plagioclase rims occur on some alkali feldspar crystals and are absent on others. The proportion of phenocrysts is essentially constant from the contact of the granite to the gabbro (Fig. 3). This lack of modal variation, the variable degree of reaction of adjacent phenocrysts, and the presence of small chilled mafic inclusions all indicate that this porphyry was well stirred.

The 2 m thick felsic dike contains bands of radiating (spherulitic) sprays of sodic plagioclase within a few centimeters of dike contacts. The inner parts of the radiating sprays have interstitial quartz, whereas the outer parts of the plagioclase laths are included in more equant, poikilitic quartz, perthitic alkali-feldspar, biotite and hornblende. Abundant minute acicular apatite needles and equant Fe–Ti oxides are abundant in the spherulites and largely absent within coarser quartz crystals that occur outside of the spherulites. Areas interstitial to the spherulites consist mainly of small equant grains of perthitic alkali-feldspar and biotite.

The hybrid felsic porphyry differs mainly in having variable amounts of very fine-grained enclaves (typically <1 cm in diameter) and corroded phenocrysts with more abundant and thicker reaction rims.

Gabbroic rocks, including the gabbroic pillows in the composite dike, have massive textures and range from very fine- to medium-grained with tabular, normally zoned plagioclase ($An_{70–35}$), augite, olivine and Fe–Ti oxides. Chilled rocks are characterized by basaltic textures with radiating sprays of plagioclase of high aspect ratio. Some chilled rocks have spherulitic intergrowths of plagioclase and olivine. Hornblende and biotite are minor phases in most gabbroic rocks. Biotite and hornblende are locally the dominant mafic phases where gabbro is strongly chilled and in contact with porphyry. In the coarser-grained interior of the gabbroic dike, plagioclase up to 2 mm in length occurs with smaller equant olivine and poikilitic augite up to 4 mm in diameter. Finer-grained areas with spherulitic intergrowths of plagioclase and olivine occur locally in these coarser gabbros.

Hybrid mafic rocks typically have fine-grained, granular textures dominated by plagioclase ($An_{50–25}$) and hornblende with varying amounts of biotite and Fe–Ti oxides, and contain some finer-grained mafic clots. Xenocrysts of quartz, sodic plagioclase ($An_{25–20}$) and alkali feldspar are heterogeneously distributed and typically in the range of 5–15 modal %.

MINERAL CHEMISTRY

Feldspars and biotite from two granite and two porphyry samples were analyzed by microprobe (Tables 2 and 3) and LA-ICP-MS (Tables 4 and 5) to compare their major and trace element compositions. Plagioclase feldspars in both granite and porphyry have similar ranges in % An ($An_{30–18}$) (Table 2). Both feldspars have moderate compositional zoning in trace elements, with most variation occurring in narrow rims. All analyses of trace elements reported in Table 4 were obtained from homogeneous to weakly zoned crystal cores. Although the number of samples is small, and whole-rock chemical variation suggests that mineral compositions could vary greatly, especially in trace elements, feldspars and biotites from these four rocks generally have similar compositional ranges. Plagioclase and alkali feldspar in the granite and porphyry samples have comparable abundances of Rb, Sr, Ba, Ga, and Pb (Table 4) as well as similar abundances and patterns of rare earth elements (REE; Fig. 9a and b). There are no significant compositional differences between biotite in the granite and the porphyry (Tables 3 and 5), and REE abundances and patterns are also comparable (Fig. 9c).

WHOLE-ROCK GEOCHEMISTRY

Thirty-five samples from the Vinal Cove complex and surrounding Vinalhaven granite, listed in Table 1, were

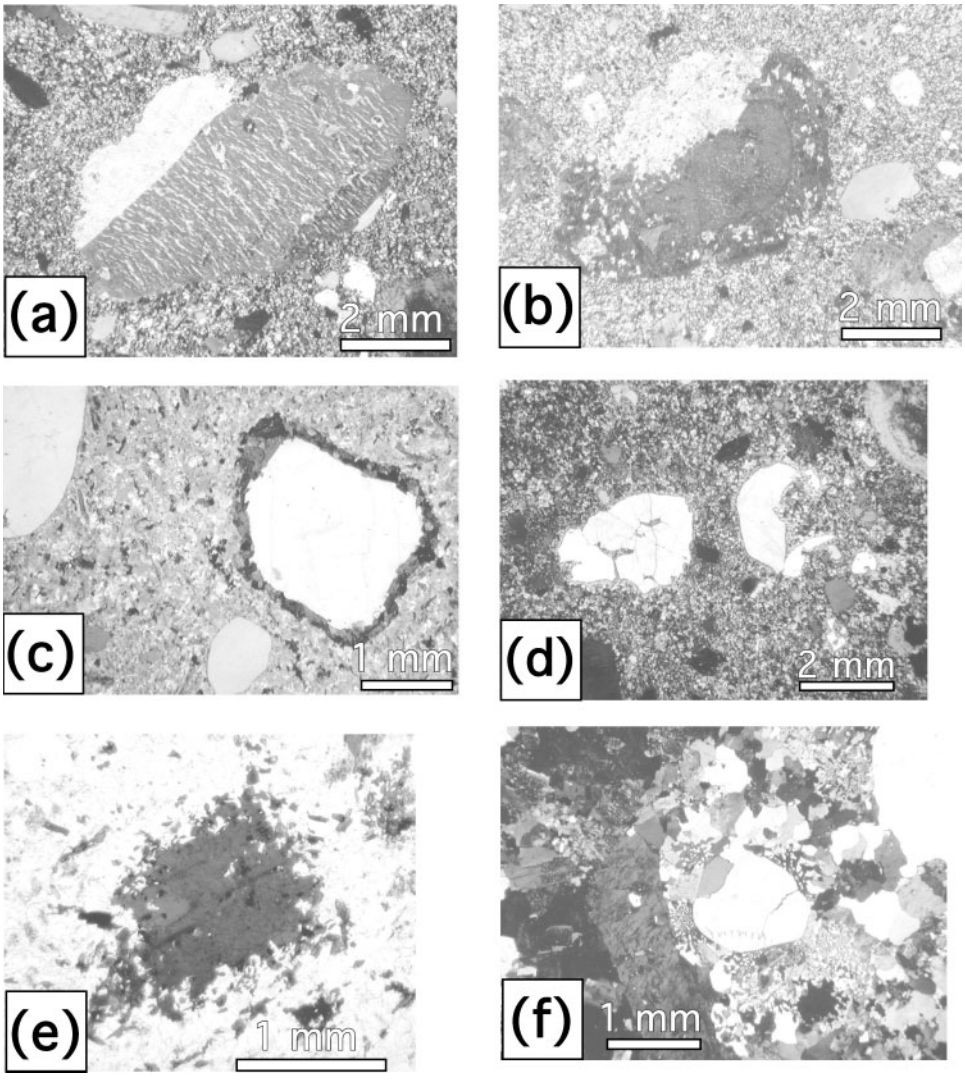

Fig. 8. Photomicrographs of corroded and reacted phenocrysts and matrix in porphyry. (a) Anhedral phenocryst of perthitic alkali-feldspar. (b) Anhedral phenocryst of alkali-feldspar with prominent rim of plagioclase containing many patches of granophyre, which probably crystallized from trapped silicic melt. (c) Three, anhedral, rounded quartz phenocrysts. It should be noted that adjacent crystals may either have or lack mafic rims. (d) Irregularly resorbed quartz phenocrysts that lack mafic rims and show optically continuous overgrowths into the matrix. (e) Anhedral biotite, which appears to have been partly resorbed. During subsequent cooling, regrowth occurred contemporaneous with matrix crystallization. (f) Prominent areas of granophyre in the fine-grained matrix of phenocryst-rich porphyry.

analyzed by XRF for major and trace elements (Table 6). Rocks that make up the Vinal Cove complex range from about 47 to 76 wt % SiO_2 and are strongly bimodal in composition (Table 6; Fig. 10), a characteristic of the Vinalhaven intrusive complex as a whole (Mitchell & Rhodes, 1989). All rocks between 51 and 67 wt % SiO_2 present clear petrographic evidence of hybridization.

Gabbroic rocks form a tight cluster of compositions on Harker diagrams, comparable with, but much more restricted than the full range of gabbros in the Vinalhaven intrusion (Fig. 10). MgO varies only between about 8 and 9 wt %. Several major and trace elements (MgO, FeO_T, TiO_2, Ni, Cr, and V) decrease with increasing SiO_2, consistent with minor fractionation of olivine, augite and Fe–Ti oxides. The compositions of these fine-grained gabbros probably approximate liquids and are typical of low-K tholeiites that are contemporaneous with granites elsewhere in the Maine magmatic province (Wiebe, 1993b). The lowest values in wt % K_2O (0·14–0·25) and ppm Rb (4–7) occur in rocks with the least amount of hornblende and biotite, and probably represent the least contaminated compositions.

On most major element Harker diagrams, the coarse-grained Vinalhaven granite samples form tight compositional groups between 73 and 75 wt % SiO_2 (Fig. 10). Although there is a tendency for MgO, CaO and a few

Table 4: Representative trace element analyses of feldspar cores from the coarse-grained Vinalhaven granite and Vinal Cove porphyry

	Plagioclase feldspar in porphyry				Plagioclase feldspar in Vinalhaven granite			
Sample:	MM-46	MM-46	MM-53	MM-53	MM-62A	MM-62A	V-002	V-002
Ga	36	37	32	32	34	34	40	38
Rb	3·6	3·5	3·2	3·0	1·3	1·4	2·3	5·1
Sr	155	147	119	129	192	204	148	110
Cs	—	—	—	0·08	—	—	—	0·28
Ba	108	71	50	44	82	127	72·9	30·0
La	18·8	17·3	17·1	17·3	21·9	21·1	21·7	19·7
Ce	23·7	21·3	23·0	23·6	29·8	29·2	29·6	26·5
Pr	2·01	1·68	1·81	1·73	2·29	2·32	2·25	2·00
Nd	5·97	5·26	5·43	5·29	7·04	7·24	5·96	5·52
Sm	0·55	0·68	0·53	0·49	0·74	0·88	0·75	0·64
Eu	2·32	1·98	1·77	2·07	2·25	2·62	2·03	1·59
Gd	—	—	0·32	0·23	0·39	0·34	—	0·42
Tb	0·036	0·031	0·028	0·031	—	0·046	0·053	0·068
Ho	0·042	0·019	0·022	0·017	—	0·019	—	—
Er	0·072	—	0·020	0·024	—	0·037	0·069	0·047
Tm	—	—	0·002	0·005	—	—	—	—
Yb	0·082	0·008	0·010	0·006	0·031	0·033	0·028	—
Lu	—	—	0·001	0·003	—	0·008	—	—
Pb	17·0	17·0	17·2	16·8	20·5	19·6	17·9	19·3

	Alkali feldspar in porphyry				Alkali feldspar in Vinalhaven granite			
Sample:	MM-46	MM-46	MM-53	MM-53	MM-62A	MM-62A	V-002	V-002
Ga	21	21	21	21	21	21	21	21
Rb	445	482	643	510	522	547	397	404
Sr	106	122	189	94	85	90	110	81
Y	0·34	—	—	0·17	0·05	0·15	0·06	—
Cs	8·6	2·2	6·7	7·9	10·8	2·8	0·98	1·6
Ba	1393	1896	3310	171	882	451	1376	1144
La	7·73	4·49	5·44	4·70	4·13	3·62	5·52	3·43
Ce	5·92	3·34	3·79	4·07	3·16	3·58	4·24	2·58
Pr	0·36	0·18	—	0·37	0·21	0·30	0·17	0·12
Nd	0·80	0·34	0·75	0·44	0·46	0·53	—	0·19
Sm	0·09	0·12	0·11	0·16	0·11	—	—	—
Eu	1·70	1·72	1·95	1·26	1·28	1·16	2·00	1·09
Gd	—	—	—	—	0·074	0·046	—	—
Tb	0·008	0·016	—	—	0·002	—	—	0·010
Ho	—	0·003	—	0·005	0·003	0·005	0·002	0·019
Er	—	—	0·015	0·026	—	0·031	0·007	0·025
Tm	—	0·023	—	0·010	—	—	—	0·027
Yb	0·057	0·069	—	0·052	0·008	—	0·024	0·011
Lu	—	0·008	—	—	—	0·002	—	0·002
Pb	37	42	86	34	50	49	47	38

—, below detection limit

Table 5: Representative trace element analyses of biotite cores from the coarse-grained Vinalhaven granite and Vinal Cove porphyry

	Biotite in porphyry				Biotite in Vinalhaven granite			
	MM-46	MM-46	MM-53	MM-53	MM-62A	MM-62A	V-002	V-002
Sc	23	19	17	17	43	34	97	101
Ga	70	63	64	59	59	56	59	59
Rb	1636	1474	1436	1511	940	930	1341	1114
Sr	2·76	—	—	—	—	1·18	—	1·09
Y	1·34	0·58	1·91	0·76	0·38	0·66	0·35	4·23
Zr	3·04	1·01	0·66	0·58	0·45	2·06	1·99	2·01
Nb	112	99	71	69	96	125	98	98
Cs	92	68	45	88	21	26	246	41
Ba	214	217	170	169	79	65	159	314
La	2·97	1·06	4·90	2·74	1·01	1·17	—	0·96
Ce	8·61	2·61	6·28	2·96	1·44	1·53	—	2·00
Nd	4·10	1·62	3·57	1·59	1·38	1·28	0·24	1·55
Sm	0·81	0·32	0·42	0·20	—	—	—	—
Eu	—	—	—	—	—	—	—	—
Tb	0·055	0·023	0·060	—	—	0·043	—	—
Ho	0·065	0·027	0·056	0·035	0·028	0·050	0·025	—
Tm	—	0·020	0·032	—	—	—	0·069	—
Yb	0·439	0·155	0·093	0·093	—	0·237	0·036	0·501
Lu	0·064	0·034	0·024	—	0·010	0·033	0·040	0·103
Tl	13·0	11·9	11·9	11·3	6·6	6·3	8·0	6·9
Pb	11·2	4·3	14·9	3·3	3·4	4·4	2·4	6·4
Th	0·65	0·094	0·021	0·021	0·03	0·11	—	—
U	3·96	0·94	1·09	0·11	0·14	0·52	—	—

—, below detection limit

other major elements to decrease as SiO_2 increases, substantial variations in trace element abundances do not obviously correlate with the small variation in wt % SiO_2. Plots of several trace elements, notably Ce, Y, Ba, and Rb, display large variations at essentially constant SiO_2. The felsic porphyries are nearly identical in composition to the Vinalhaven granite (Fig. 10). They range in SiO_2 from about 73 to 76 wt %, and have comparable variations in major and trace elements. Fine-grained granite from the composite dike plots nearly at the high-SiO_2 end of trends defined by coarse-grained granite and porphyry on most Harker diagrams (Fig. 10). All of these felsic rocks have compositions that lie close to the 1 kbar minimum in the system SiO_2–Ab–Or–H_2O.

In Harker diagrams, hybrid felsic and mafic rocks define essentially linear trends (for all major and trace elements) that are close to linear mixing lines between average gabbroic and granitic rocks (Fig. 10). The felsic hybrid rocks appear to be only slightly displaced toward higher concentrations of Na_2O and Y, and the mafic hybrid rocks toward higher concentrations of Ba and Na_2O and lower Ga. The felsic hybrid rocks define a continuous trend from the felsic porphyries down to about 66 wt % SiO_2. These trends are largely consistent with petrographic evidence for direct mixing of small mafic clots into the felsic porphyry. The hybrid mafic rocks define linear trends from about 55 to 60 wt % SiO_2, consistent with the presence of small percentage of quartz and feldspar xenocrysts. The compositional gap between the gabbros and the hybrid mafic rocks may reflect inadequate sampling. Rocks with whole-rock compositions between the mafic and felsic hybrid rocks (between about 60 and 66 wt % SiO_2) appear to be absent.

DISCUSSION

Origin of the Vinal Cove porphyry

The rocks of the Vinal Cove complex appear to record events during the waning stages of solidification of the

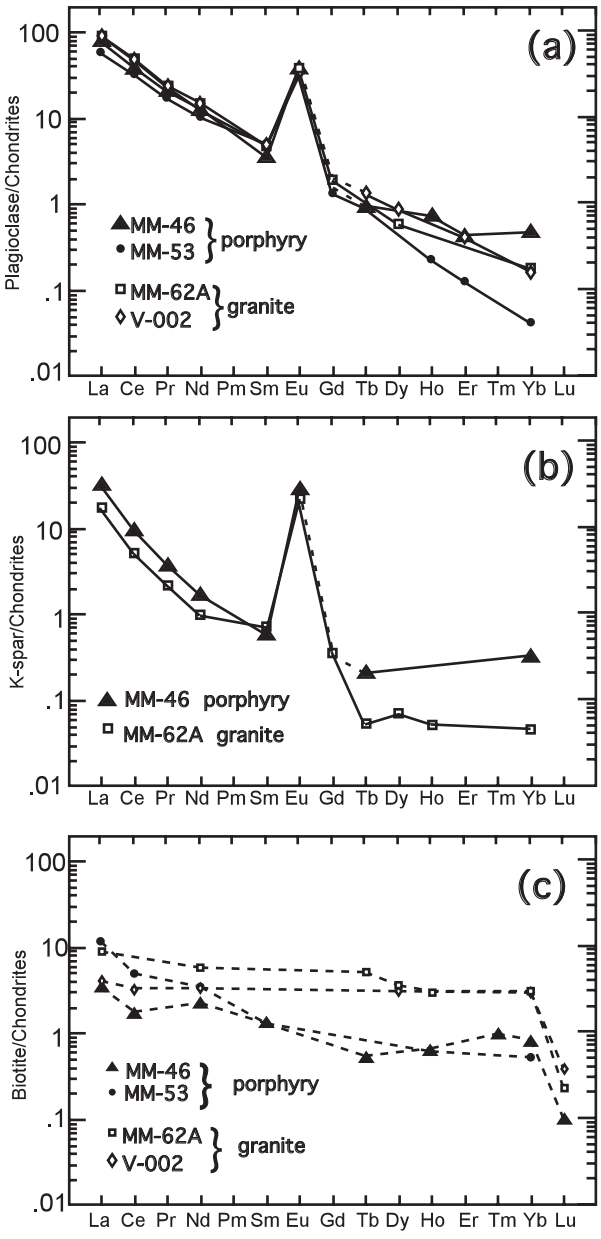

Fig. 9. Plots of REEs in mineral cores from samples of the Vinalhaven granite and the Vinal Cove porphyry, determined by LA-ICP-MS. (a) Plagioclase; (b) alkali feldspar; (c) biotite. The close similarity of concentrations and patterns in feldspars and biotite from the granite and the porphyry should be noted.

Vinalhaven intrusive complex, when a large, mafic dike intruded a small, partially molten, inner portion of the mostly solidified, coarse-grained Vinalhaven granite.

Field and petrographic relations provide abundant evidence that basalt, porphyry, and granite coexisted in the Vinal Cove complex as contemporaneous magmas capable of commingling and limited mixing. Although the basaltic dike cuts the Vinalhaven granite sharply for most of its length, basalt grades to hybrid mafic rocks in a central segment several hundred meters in length, and these hybrid mafic rocks commingle with felsic porphyry along the northern contact of the dike. Xenocrysts of quartz and feldspar in mafic hybrid rocks and small mafic to intermediate enclaves and hornblende in hybrid felsic porphyry indicate that some mixing occurred above the two solidi. Contacts between the Vinalhaven granite and the main area of the Vinal Cove porphyry do not cut across crystals in the granite or porphyry, are commonly gradational over several centimeters, and are commonly highly irregular with complex zones of commingling between granite and porphyry. Thus, both the porphyry and granite were mobile when they came into contact. In other areas, however, porphyry dikes that extend as far as 2 km east of the main body cut sharply across crystals in the cg granite, reflecting brittle deformation in areas away from the main body of the Vinal Cove porphyry.

We propose that the porphyry formed largely by remelting and remobilization of Vinalhaven granite. The whole-rock composition of the porphyry is identical to that of the Vinalhaven granite and carries corroded phenocrysts with major and trace element compositions that closely match minerals of the enclosing granite. Although resorption of phenocrysts in the porphyry might be explained by decompression during emplacement of new granitic magma (undersaturated in H_2O), the highly variable resorption and reaction shown by adjacent phenocrysts is inconsistent with decompression and implies thorough mixing of magma and crystals after a resorption event that affected phenocrysts to varying degrees. The existence of weakly corroded biotite phenocrysts in the porphyry indicates that dehydration melting was not important and, hence, requires that the Vinalhaven granite contained hydrous interstitial melt prior to rejuvenation. Within the area mapped as crystal-poor porphyry, the occurrence of some areas of fine-grained granite that lack corroded phenocrysts suggests that some new felsic magma (represented by fine-grained granite in a composite dike) may also have contributed to the body of porphyry.

These relationships are most consistent with the emplacement of basaltic magma as a steep dike into an incompletely solidified volume of the coarse-grained Vinalhaven granite (Fig. 11). The area of heterogeneous mafic hybrid rocks was probably produced at the point where the basalt intersected this volume, causing the basalt to stall, spread laterally, and underplate a zone of crystal mush (Fig. 11b). Upward transfer of heat from the basalt may initially have been largely conductive, but as remelting of crystal mush proceeded, convective transport should have become important (Couch *et al.*, 2001). This convective movement would have mixed melt and strongly resorbed crystals from a thermal boundary layer upward into cooler crystal mush, explaining the highly

Table 6: Representative whole-rock chemical compositions of the coarse-grained Vinalhaven granite and rocks from the Vinal Cove complex

Type:	Coarse-grained Vinalhaven granite							Gabbroic rocks				
Details:								mg	chill	chill	chill	dike
Sample	MM-3	MM-41	MM-44A	MM-62A	V2-42C	V2-1	V2-2	MM-69	MM-7	V2-42A	MM-4	V2-6
SiO_2	73·62	73·62	72·61	74·06	73·44	73·71	73·55	47·09	47·13	47·40	48·20	48·76
TiO_2	0·33	0·31	0·37	0·34	0·34	0·26	0·39	1·57	1·83	1·39	1·75	1·43
Al_2O_3	13·04	13·12	13·53	13·05	12·92	12·93	13·08	16·59	16·31	16·60	16·28	16·69
Fe_2O_3	2·25	2·18	2·40	2·18	2·28	1·75	2·36	11·35	11·93	10·33	11·50	10·41
FeO	0·00	0·00	0·00	0·00	0·00	0·00	0·00	0·00	0·00	0·00	0·00	0·00
MnO	0·06	0·05	0·05	0·05	0·03	0·05	0·05	0·19	0·19	0·18	0·19	0·17
MgO	0·48	0·42	0·52	0·42	0·50	0·35	0·51	8·74	8·43	8·35	8·23	7·90
CaO	1·13	1·14	1·22	1·05	1·27	0·97	1·21	11·05	10·39	10·57	10·07	10·29
Na_2O	3·22	3·26	3·26	3·24	3·03	3·33	3·25	2·81	2·94	2·56	2·92	2·80
K_2O	5·09	5·08	5·33	5·02	4·74	4·84	4·88	0·14	0·25	0·58	0·41	0·49
P_2O_5	0·08	0·08	0·11	0·09	0·10	0·07	0·09	0·16	0·22	0·17	0·21	0·15
LOI	0·37	0·28	0·37	0·40	0·68	0·36	0·39	0·34	0·03	0·99	0·20	0·20
Total	99·67	99·52	99·76	99·89	99·32	98·61	99·77	100·02	99·65	99·12	99·95	99·28
Ba	311	306	329	284	268	302	315	34	52	44	57	59
Rb	200	202	209	197	158	264	203	4	7	28	16	22
Sr	49	47	54	48	66	39	51	225	220	217	219	211
Pb	20	22	23	20	25	23	21	3	4	9	4	5
Th	15·6	18·0	19·8	8·8	20·0	22·4	16·6	0·3	1·0	0·7	1·6	1·1
U	4·0	5·4	3·3	3·8	4·9	7·5	2·2	0·6	0·6	0·0	0·3	0·1
Zr	183	189	215	190	186	169	198	98	137	100	136	101
Nb	11·0	11·1	11·5	12·1	11·7	14·3	12·1	2·9	4	3·4	4·3	3·7
Y	45	45	42	37	34	59	44	29	33	27	32	29
V	33	30	35	34	35	24	35	227	256	242	239	222
Cr	15	8	17	7	11	12	15	233	272	268	282	212
Ni	4	2	3	3	3	2	4	141	142	134	147	106
Zn	38	32	31	31	29	30	33	68	77	74	76	68
Ga	17·1	17·5	17·1	16·9	17·1	17·4	16·6	16·5	17·5	15·2	17·5	16·6
Ce	91·1	85·3	80·1	76·0	58·4	86·8	56·6	10·9	15·4	12·1	15·9	16·4
La	47·6	42·4	38·0	22·2	27·7	37·8	26·1	4·3	6·7	4·0	5·7	5·9
Co	4	4	5	4	4	4	4	44	46	42	44	40
Cu	0	0	0	0	5	2	2	53	51	64	49	54
Sc	7	7	7	8	8	7	6	31	33	40	33	31

Table 6: continued

Rock type:	Composite dike		Mafic hybrid rocks				Hybrid porphyry			
Details:	Basalt	fg granite								
Sample:	MM-6B	MM-6A	V2-13A	MM-68A	MM-68B	V2-13B	MM-68C	MM-5	MM-8B	MM-68D
SiO_2	49·64	74·99	54·45	57·29	58·32	59·10	66·46	68·52	70·43	71·30
TiO_2	1·29	0·18	1·39	1·30	1·14	1·14	0·77	0·63	0·51	0·48
Al_2O_3	16·56	13·26	15·08	14·95	14·62	14·94	13·92	13·83	13·62	13·34
Fe_2O_3	9·90	1·42	8·97	8·39	7·55	7·42	4·87	4·13	3·44	3·13
FeO	0·00	0·00	0·00	0·00	0·00	0·00	0·00	0·00	0·00	0·00
MnO	0·17	0·04	0·15	0·14	0·14	0·13	0·10	0·08	0·06	0·07
MgO	7·94	0·32	5·62	5·17	4·85	4·52	2·35	1·94	1·01	1·08
CaO	10·33	0·88	7·46	6·66	6·32	5·96	3·62	2·89	2·04	1·97
Na_2O	2·89	3·43	2·99	3·07	3·20	3·09	3·35	3·37	3·54	3·33
K_2O	0·58	4·93	1·67	2·05	2·18	2·28	3·62	3·83	4·30	4·52
P_2O_5	0·16	0·07	0·18	0·17	0·14	0·16	0·12	0·11	0·10	0·09
LOI	0·35	0·52	0·74	0·73	0·59	0·80	0·39	0·53	0·43	0·35
Total	99·81	100·04	98·70	99·93	99·05	99·54	99·56	99·87	99·48	99·65
Ba	60	379	146	171	201	211	216	271	239	256
Rb	27	244	73	92	101	107	171	175	188	203
Sr	202	54	169	165	153	142	92	89	70	63
Pb	5	26	10	12	14	13	16	19	19	19
Th	1·8	17·3	6·7	9·1	9·0	9·3	14·8	13·9	17·7	17·6
U	0·8	7·7	2·8	3·1	2·5	2·6	4·0	3·8	4·4	6·1
Zr	101	138	124	123	119	130	153	137	190	158
Nb	4·2	11·9	6·9	7·3	7·2	8·0	9·8	11·2	11·4	11·1
Y	26	35	34	34	33	37	40	37	49	46
V	205	19	206	191	174	176	103	81	56	53
Cr	230	10	162	184	166	155	70	63	22	29
Ni	128	2	81	74	70	70	27	23	8	10
Zn	66	19	67	63	58	60	51	40	41	37
Ga	15·9	16·1	16·5	16·2	16·1	16·1	16·7	16·8	18·1	17·7
Ce	16·2	54·3	34·4	35·5	35·5	43·8	53·5	48·8	53·1	55·1
La	4·3	26·1	12·6	14·3	14·4	19·1	25·6	19·8	24·0	21·7
Co	41	2	28	26	24	24	13	10	6	6
Cu	48	0	41	26	22	43	2	0	0	0
Sc	32	4	29	27	24	25	15	14	11	7

Type:	Porphyry													
Sample:	V2-8	MM-36	V2-42B	MM-62B	V2-7	MM-46	MM-57	MM-63	MM-2	V2-41	V2-13C	MM-67	MM-8A	MM-53
SiO_2	71·23	73·05	72·02	73·17	72·62	72·92	73·31	73·03	73·16	72·50	74·65	75·11	75·94	72·17
TiO_2	0·36	0·36	0·38	0·37	0·32	0·35	0·31	0·35	0·36	0·37	0·31	0·20	0·13	0·40
Al_2O_3	13·18	13·30	13·12	13·21	13·25	13·14	13·52	13·32	13·17	12·89	13·27	13·16	12·98	13·34
Fe_2O_3	2·42	2·54	2·50	2·39	2·38	2·37	2·09	2·24	2·39	2·42	2·13	1·43	1·23	2·73
FeO	0·00	0·00	0·00	0·00	0·00	0·00	0·00	0·00	0·00	0·00	0·00	0·00	0·00	0·00
MnO	0·06	0·05	0·06	0·05	0·07	0·05	0·05	0·05	0·05	0·07	0·05	0·04	0·02	0·06
MgO	0·81	0·66	0·72	0·71	0·74	0·61	0·60	0·54	0·59	0·59	0·57	0·30	0·18	0·85
CaO	1·45	1·39	1·55	1·37	1·34	1·32	1·35	1·28	1·34	1·28	1·28	0·94	0·77	1·69
Na_2O	3·14	3·33	3·22	3·29	3·26	3·24	3·30	3·43	3·35	3·15	3·18	3·31	3·36	3·32
K_2O	4·85	4·83	4·52	4·90	4·63	4·98	4·97	4·86	4·83	4·90	4·98	5·00	5·16	4·65
P_2O_5	0·09	0·08	0·09	0·08	0·08	0·08	0·08	0·08	0·09	0·08	0·08	0·06	0·04	0·09
LOI	0·63	0·34	0·43	0·41	0·55	0·34	0·47	0·37	0·33	0·40	0·42	0·31	0·27	0·00
Total	98·21	99·92	98·59	99·94	99·23	99·39	100·05	99·56	99·66	98·66	100·92	99·85	100·07	99·30
Ba	313	300	261	296	301	303	348	308	294	289	318	305	206	286
Rb	224	224	184	232	261	231	221	204	214	214	227	252	236	201
Sr	63	55	57	53	51	53	58	53	52	50	52	44	34	58
Pb	22	22	22	22	20	23	22	20	21	19	22	27	23	22
Th	20·6	21·3	19·1	18·0	20·7	19·5	20·2	21·1	20·0	19·5	31·2	17·6	19·3	17·1
U	4·1	4·8	4·3	5·1	5·3	4·2	5·1	3·4	5·0	5·4	3·9	5·8	5·0	4·5
Zr	160	167	167	172	143	164	165	170	179	184	153	135	116	161
Nb	11·3	11·7	11·6	11·5	12·1	11·7	12·0	11·2	12·0	11·9	11·1	11·9	12·0	11·6
Y	40	48	48	44	42	43	43	44	46	47	41	34	37	49
V	42	37	41	38	38	37	33	34	31	35	30	13	10	44
Cr	31	17	21	39	25	17	45	22	19	12	12	19	22	33
Ni	7	5	6	5	7	4	5	4	4	4	4	1	1	9
Zn	33	31	34	32	41	29	31	33	36	40	30	19	14	33
Ga	16·3	17·9	17·7	17·4	16·9	17·2	17·1	17·3	17·9	17·2	16·1	16·3	16·3	16·8
Ce	90·2	103·3	61·6	72·9	48·8	35·6	87·3	91·1	70·7	64·0	91·7	59·2	29·6	102·5
La	49·1	53·1	29·4	35·4	14·1	14·7	45·6	31·6	28·8	20·7	45·9	28·3	10·8	56·6
Co	4	6	5	5	5	5	4	4	5	5	4	3	3	6
Cu	2	0	0	0	0	0	0	0	0	1	3	0	0	2
Sc	7	6	9	6	8	6	6	8	8	8	8	6	3	8

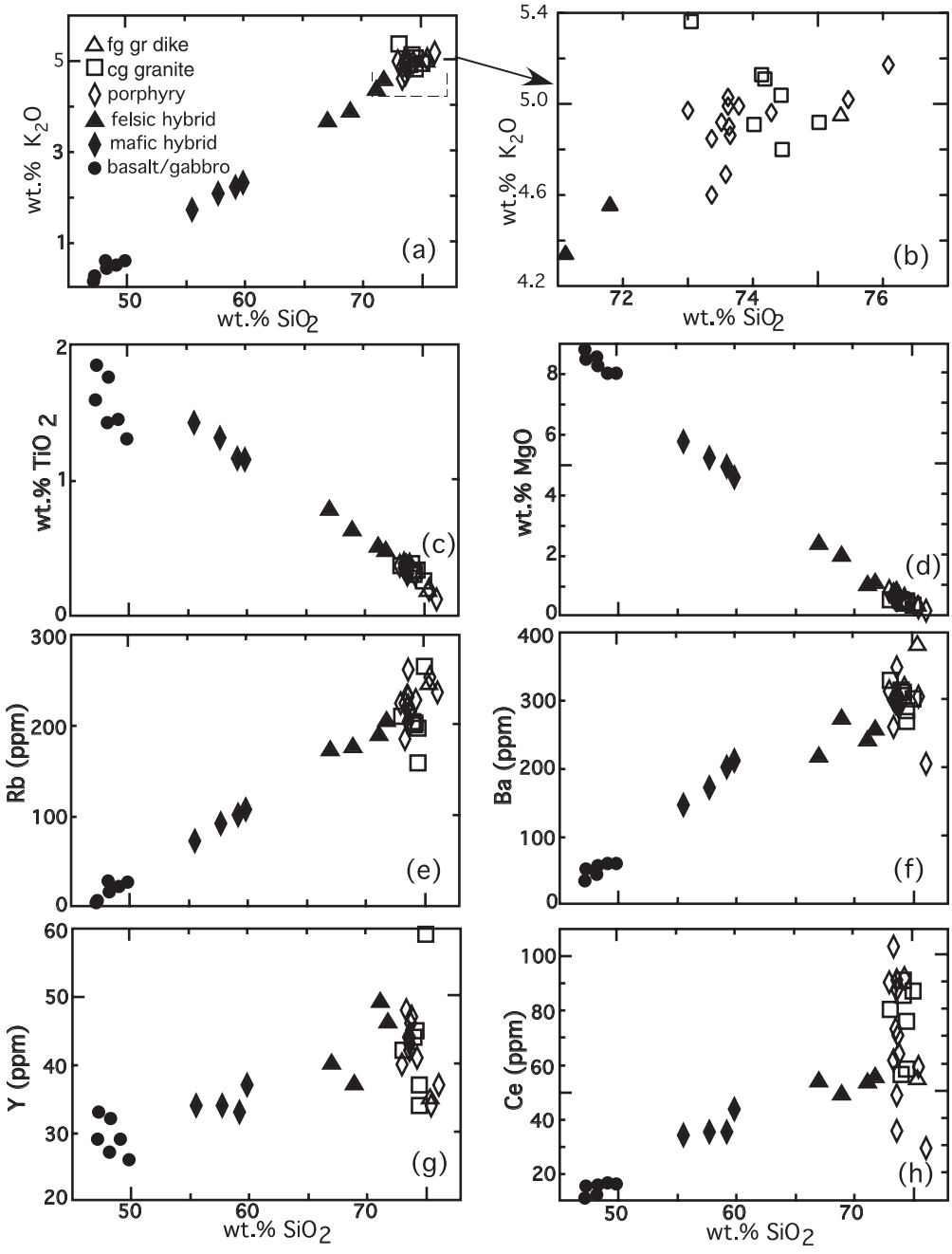

Fig. 10. Plots of selected major and trace elements against wt % SiO_2 for rocks from the Vinal Cove complex and enclosing coarse-grained Vinalhaven granite. The felsic porphyries are nearly identical in composition and in compositional range to the Vinalhaven granite. Mafic and felsic hybrid rocks from the Vinal Cove complex form a linear array for all elements between chilled mafic rocks and the granite/porphyry.

contrasted resorption and reaction shown by adjacent phenocrysts throughout the porphyry. A process essentially identical to this (convective self-mixing) has been proposed to explain similar petrographic relations in recently erupted andesites from the Soufriere Hills volcano, Montserrat (Murphy *et al.*, 2000; Couch *et al.*, 2001).

Role of basalt in producing the porphyry

The ~20 cm thick zone of porphyry between Vinalhaven granite and basalt (at locality V2-42) indicates that, at least locally, the basaltic magma provided the thermal energy for remelting Vinalhaven granite. Microgranular zones along quartz–feldspar grain contacts in granite

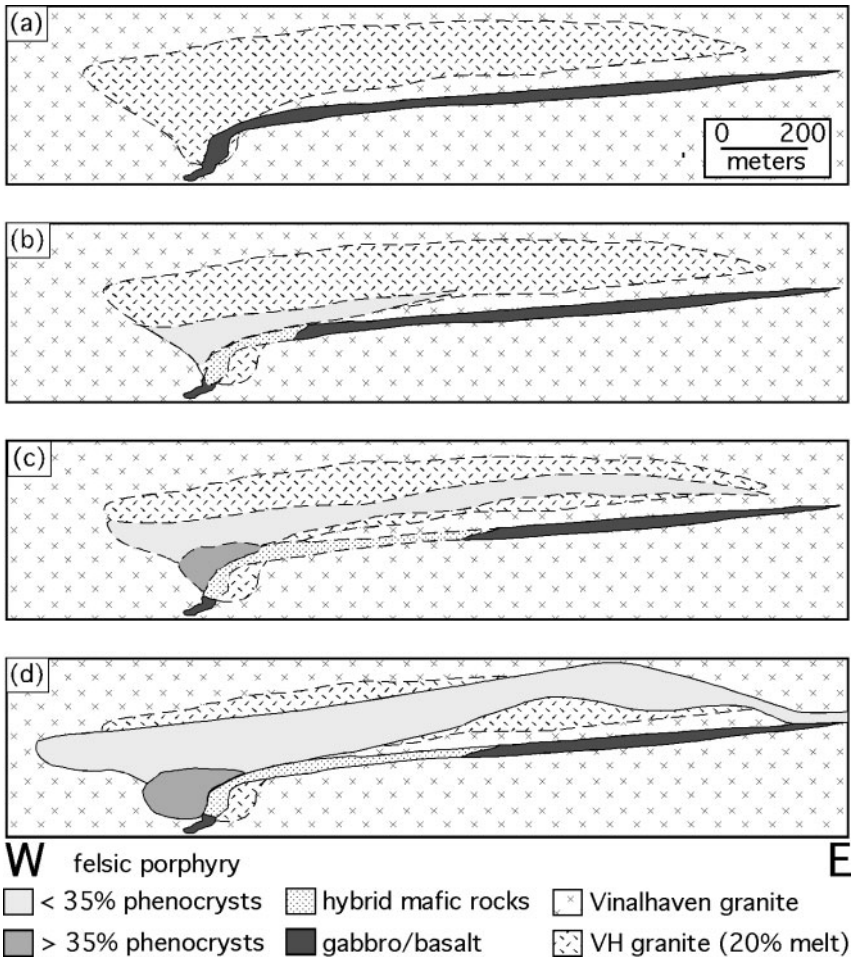

Fig. 11. Schematic east–west sections to illustrate the probable evolution of the Vinal Cove complex (a, initial state; d, final state). Because the Vinalhaven intrusion is tilted gently to the north, the map of the Vinal Cove complex (Fig. 2) can be viewed as an oblique section through the complex. Section (d) is roughly equivalent to a downdip view (~20°N) of the complex. (a) Hypothetical initial state of the granite when the basaltic dike was emplaced. (b) Early development of hybrid rocks where the basalt intersected partially molten granite. Growth of crystal-poor thermal boundary layer above mafic hybrid rocks. (c) Continued growth of the volume of phenocryst-poor porphyry and initial formation of crystal-rich porphyry at the base as a result of crystal accumulation. (d) Final state of the Vinal Cove complex.

contiguous with this porphyry appear to represent crystallization of melt films that formed as a result of heat transferred from the basalt and porphyry. The well-mixed character of the porphyry layer suggests that it did not form in place, but developed by melting granite along the margin of the basalt. Felsic melt that was generated then probably continued to flow with the basalt and mix internally until the basalt margin solidified.

On a larger scale, the occurrence of a contiguous zone of hybrid mafic rocks and hybrid felsic porphyries between the Vinal Cove porphyry and the basaltic dike (Fig. 2) and the occurrence of tiny mafic enclaves in the porphyry leave little doubt that crystallization and cooling of the basalt contributed heat for melting Vinalhaven granite to produce the porphyry. Contacts between the granite and the porphyry and the presence of weakly corroded biotite phenocrysts in the porphyry suggest that the Vinalhaven granite in this area must have had interstitial hydrous melt (perhaps 10–30%) when the basaltic dike was emplaced.

Because the tholeiitic basaltic magma appears to have been relatively dry, crystallizing hornblende prominently only where basalt comes in contact with hydrous granitic magma, the basalt could have provided little additional water to aid melting. On the contrary, the anomalous hydrous character of chilled mafic magma where it has commingled with porphyry (e.g. Fig. 3) suggests that growth of hydrous phases (hornblende and biotite) in the basalt may have dehydrated the porphyry magma.

Although it is impossible to constrain closely the relative volumes of basalt and porphyry or, indeed, the 3-D spatial arrangement of basalt and porphyry, outcrop-scale features in hybrid mafic rocks suggest that, where

the basaltic dike encountered a volume of granite with, perhaps, 20% interstitial melt, it spread laterally to the north to produce a gently northward-dipping, sheet-like body that now underlies the porphyry. Upward transfer of heat from this mafic sheet may initially have been largely conductive, but production of a buoyant boundary layer would have led to convection (Couch *et al.*, 2001). To evaluate whether crystallization and cooling of basalt could provide enough heat to generate the porphyry, we assumed basalt with an initial temperature of 1200°C, latent heats of 70 cal/g (granite) and 100 cal/g (basalt), and a specific heat of 0·28 cal/g for both granite and basalt. If Vinalhaven granite along this segment of the basaltic dike initially contained about 20% melt at 775°C, crystallization and cooling of 1 g of basalt from 1200°C to 775°C would have provided enough heat to generate ~3·5 g of Vinalhaven granite at 775°C with 80% melt (= porphyry). Although the mass ratio is only about half the areal ratio (about 1:7) of mafic to felsic rocks in the Vinal Cove complex, field relations do suggest that a sheet-like mass of mafic material lies beneath the porphyry, and, therefore, that convective heat transfer from cooling the basalt could have thermally rejuvenated the granite to produce all of the porphyry.

Remelting of the granite need not have produced all of the porphyry magma. Fine-grained granite and chilled mafic pillows (identical in composition to the main basaltic dike) occur within a composite dike that cuts the hybrid mafic rocks (near location 4 in Fig. 2). Comparable dikes are unknown within the interior of the Vinalhaven granite, but are common in the gabbro–diorite unit. The composition of the granitic component of this dike is essentially indistinguishable from the most silicic and phenocryst-poor rocks in the northern area of the porphyry (Table 6; Fig. 10). The occurrence of this composite dike indicates that some new silicic magma was emplaced along with additional basaltic magma shortly following the emplacement of the large basaltic dike. This new silicic magma could also have contributed to the volume of the porphyry.

Cause of plutonic quenching

There is widespread evidence for a late stage of rapid crystallization throughout much of the Vinal Cove porphyry as well as in thin zones of apparent melt films between quartz and feldspar in some of the enclosing Vinalhaven granite. Microgranophyric textures are widespread in the porphyry matrix, and micrographic overgrowths on corroded phenocrysts are commonly well developed. The ~20 cm thick zone of porphyry 'sandwiched' between the granite and the chilled margin of basalt has a granophyric matrix that is so fine-grained that it may partly have originated by devitrification. The micrographic textures are particularly fine-grained in dikes that emanate from the main body of porphyry, and one dike extending to shallower depths displays well-developed spherulites of sodic plagioclase. In this environment (1–2 kbar and about 775°C), it seems most unlikely that quench textures preserved in the porphyry formed as a result of a rapid drop in temperature. Instead, these textures probably formed in response to a sudden drop in pressure that resulted in saturation and rapid loss of H_2O and produced rapid undercooling (Lowenstern *et al.*, 1997). The occurrence of coeval rhyolite with the Vinalhaven intrusive complex suggests that this occurrence of plutonic quenching involved eruption as well as degassing.

Plutonic and volcanic records of rejuvenation

It has long been recognized that new mafic input has commonly occurred just prior to eruption of silicic magma (e.g. Sparks *et al.*, 1977). Recent studies of several silicic volcanic systems have suggested a variety of evidence that the crystal content of magma chambers may wax and wane, possibly depending on the rate of new mafic input (Mahood, 1990). Two recent studies have provided convincing evidence that mafic replenishments did, in fact, remobilize magma chambers that even approached solidus conditions: in the small andesitic magma chamber that fed recent eruptions in Montserrat (Murphy *et al.*, 2000) and in the batholith-sized magma chamber that produced the Fish Canyon tuff in the San Juan volcanic field, Colorado (Bachmann *et al.*, 2002).

In the Vinalhaven intrusive complex, basaltic replenishments occurred at many times. Most of them appear to have ponded and spread across the base of an existing silicic magma chamber, and some replenishments appear to have triggered large stoping events that may record eruptions of magma from the chamber (Hawkins & Wiebe, in preparation). In contrast, one of the last basaltic replenishments into the Vinalhaven intrusive complex produced the Vinal Cove complex, which appears to be the plutonic record of rejuvenation of a largely solidified magma chamber. The shallow level of emplacement and the strongly chilled matrix of some of the Vinal Cove porphyry are consistent with pressure quenching of hydrous magma as a result of degassing and/or eruption of rejuvenated magma (porphyry). One goal of current field study is the search for eruptive products in coeval volcanic rocks that might record such a rejuvenation event.

ACKNOWLEDGEMENTS

We thank Olivier Bachmann, James Beard and Rod Metcalf for critical reviews that helped us to improve our presentation. Phil Piccoli provided valuable assistance

with microprobe analysis, and Richard Ash is thanked for his help with ICP-MS analysis. Research was supported by the Keck Foundation, through the Keck Geology Consortium, and by NSF Research Grants EAR-0003260 to R.A.W. and EAR-0003555 to D.P.H. The analytical work at the University of Maryland was supported by the US National Science Foundation (EAR Grants 0004128 and 0004095).

REFERENCES

Allen, S. R. (2001). Reconstruction of a major caldera-forming eruption from pyroclastic deposit characteristics: Kos Plateau Tuff, eastern Aegean Sea. *Journal of Volcanology and Geothermal Research* **105**, 141–162.

Bachmann, O., Dungan, M. A. & Lipman, P. W. (2002). The Fish Canyon magma body, San Juan Volcanic Field, Colorado: rejuvenation and eruption of an upper-crustal batholith. *Journal of Petrology* **43**, 1469–1503.

Barth, M. G., Rudnick, R. L., Horn, I., McDonough, W. F., Spicuzza, M. J., Valley, J. W. & Haggerty, S. E. (2001). Geochemistry of xenolithic eclogites from West Africa, Part I: a link between low MgO eclogites and Archean crust formation. *Geochimica et Cosmochimica Acta* **65**, 1499–1527.

Coleman, D. S., Glazner, A. F., Miller, J. S., Bradford, K. J., Frost, T. P., Joye, J. L. & Bachl, C. A. (1995). Exposure of a Late Cretaceous layered mafic-felisc magma system in the Sierra Nevada batholith, California. *Contributions to Mineralogy and Petrology* **120**, 129–136.

Couch, S., Sparks, R. S. J. & Carroll, M. R. (2001). Mineral disequilibrium in lavas explained by convective self-mixing in open magma chambers. *Nature* **411**, 1037–1039.

Govindaraju, K. (1994). 1994 compilation of working values and sample description for 383 geostandards. *Geostandards Newsletter* **18**, Special Issue, 1–158.

Hawkins, D. P., Wobus, R. A. & Wiebe, R. A. (2002). Silurian U–Pb zircon dates from the Vinalhaven intrusion and associated volcanic rocks, Penobscot Bay, Maine. *Geological Society of America, Abstracts with Programs* **34**(6), 42.

Hogan, J. P. & Sinha, A. K. (1989). Compositional variation of plutonism in the coastal Maine magmatic province: mode of origin and tectonic setting. In: Tucker, R. D. & Marvinney, R. G. (eds) *Igneous and Metamorphic Geology. Maine Geological Survey, Department of Conservation, Studies of Maine Geology* **4**, 1–33.

Keller, J. (1969). Origin of rhyolites by anatectic melting of granitic crustal rocks. *Bulletin Volcanologique* **33**, 942–959.

Lowenstern, J. B., Clynne, M. A. & Bullen, T. D. (1997). Comagmatic A-type granophyre and rhyolite from the Alid volcanic center, Eritrea, northeast Africa. *Journal of Petrology* **38**, 1707–1721.

Mahood, G. A. (1990). Second reply to comment of R. S. J. Sparks, H. E. Huppert and C. J. N. Wilson on 'Evidence for long residence times of rhyolitic magma in the Long Valley magmatic system: the isotopic record in the precaldera lavas of Glass Mountain'. *Earth and Planetary Science Letters* **99**, 395–399.

Michael, P. J. (1991). Intrusion of basaltic magma into a crystallizing granitic magma chamber: the Cordillera del Paine pluton in southern Chile. *Contributions to Mineralogy and Petrology* **108**, 396–418.

Mitchell, C. B. & Rhodes, J. M. (1989). Granite–gabbro complex on Vinalhaven Island, Maine. In: Tucker, R. D. & Marvinney, R. G. (eds) *Igneous and Metamorphic Geology. Maine Geological Survey, Department of Conservation, Studies of Maine Geology* **4**, 45–62.

Murphy, M. D., Sparks, R. S. J., Barclay, J., Carroll, M. R. & Brewer, T. S. (2000). Remobilization of andesite magma by intrusion of mafic magma at the Soufriere Hills Volcano, Montserrat, West Indies. *Journal of Petrology* **41**, 21–42.

Patrick, D. W. & Miller, C. F. (1997). Processes in a composite, recharging magma chamber: evidence from magmatic structures in the Aztec Wash pluton, Nevada. *Proceedings of the 30th International Geological Congress* **15**, 121–135.

Pitcher, W. S. (1991). Synplutonic dykes and mafic enclaves. In: Didier, J. & Barbarin, B. (eds) *Enclaves and Granite Petrology*. Amsterdam: Elsevier, pp. 383–391.

Porter, B. S., Wiebe, R. & Cheney, J. T. (1999). Regional and contact metamorphism of Paleozoic greenschist and pelites, Vinalhaven Island, Maine. *Geological Society of America, Abstracts with Programs* **31**(2), A-61.

Seaman, S. J., Wobus, R. A., Wiebe, R. A., Lubick, N. & Bowring, S. A. (1995). Volcanic expression of bimodal magmatism: the Cranberry Island–Cadillac Mountain Complex, coastal Maine. *Journal of Geology* **103**, 301–311.

Snyder, D., Crambes, C., Tait, S. & Wiebe, R. A. (1997). Magma mingling in dikes and sills. *Journal of Geology* **105**, 75–86.

Sparks, R. S. J., Sigurdsson, H. & Wilson, L. (1977). Magma mixing: a mechanism for triggering acid explosive eruptions. *Nature* **267**, 315–318.

Wiebe, R. A. (1974). Coexisting intermediate and basic magmas, Ingonish, Cape Breton Island. *Journal of Geology* **82**, 74–87.

Wiebe, R. A. (1993*a*). Basaltic injections into floored silicic magma chambers. *EOS Transactions, American Geophysical Union* **74**, 1, 3.

Wiebe, R. A. (1993*b*). The Pleasant Bay layered gabbro–diorite, coastal Maine: ponding and crystallization of basaltic injections into a silicic magma chamber. *Journal of Petrology* **34**, 461–489.

Wiebe, R. A. (1994). Silicic magma chambers as traps for basaltic magmas: the Cadillac Mountain Intrusive Complex, Mount Desert Island, Maine. *Journal of Geology* **102**, 423–437.

Wiebe, R. A. (1996). Mafic–silicic layered intrusions: the role of basaltic injections on magmatic processes and evolution in silicic magma chambers. *Transactions of the Royal Society of Edinburgh: Earth Sciences* **87**, 233–242.

Wiebe, R. A. & Collins, W. J. (1998). Depositional features and stratigraphic sections in granitic plutons: implications for the emplacement and crystallization of granitic magma. *Journal of Structural Geology* **20**, 1273–1289.

Wiebe, R. A. & Hawkins, D. P. (2003). Construction of the Vinalhaven intrusive complex, Vinalhaven Island, coastal Maine. *Geological Society of America, Abstracts with Programs* **35**(3), 36.

Wiebe, R. A., Frey, H. & Hawkins, D. P. (2001). Basaltic pillows mounds in the Vinalhaven intrusion, Maine. *Journal of Volcanology and Geothermal Research* **107**, 171–184.